SCIENCE CHINA
Information Sciences

• Supplementary File •

Distributed exact quantum amplitude amplification algorithm for arbitrary quantum states

Xu ZHOU[1*], Wenxuan TAO[2], Keren LI[3] & Shenggen ZHENG[4]

[1]*Yangtze Delta Industrial Innovation Center of Quantum Science and Technology, Suzhou 215000, China*
[2]*Shanghai MiQro Era Digital Technology Co., Ltd., Shanghai 200023, China*
[3]*College of Physics and Optoelectronic Engineering, Shenzhen University, Shenzhen 518060, China*
[4]*Quantum Science Center of Guangdong-Hong Kong-Macao Greater Bay Area (Guangdong), Shenzhen 518045, China*

Appendix A Analysis of the QAAA in subsection 2.1

After applying the unitary operator $\mathcal{A}$, we obtain

$$\begin{aligned}
|\Psi\rangle &= \mathcal{A}|0\rangle^{\otimes n} = \sum_{x\in\{0,1\}^n} \gamma_x |x\rangle && \text{(A1)}\\
&= \sum_{x\in X_g} \alpha_x |x\rangle + \sum_{x\in X_b} \beta_x |x\rangle && \text{(A2)}\\
&= \sqrt{p_g}\sum_{x\in X_g} \frac{\alpha_x}{\sqrt{p_g}}|x\rangle + \sqrt{1-p_g}\sum_{x\in X_b}\frac{\beta_x}{\sqrt{1-p_g}}|x\rangle && \text{(A3)}\\
&= \sqrt{p_g}|\Psi_g\rangle + \sqrt{1-p_g}|\Psi_b\rangle, && \text{(A4)}
\end{aligned}$$

where

$$\sin\theta = \sqrt{p_g},\ \ \cos\theta = \sqrt{1-p_g}, \tag{A5}$$

and

$$p_g = \sum_{x\in X_g} |\alpha_x|^2. \tag{A6}$$

Here, the states $|\Psi_g\rangle$ and $|\Psi_b\rangle$ are defined as

$$\begin{aligned}
|\Psi_g\rangle &= \sum_{x\in X_g} \frac{\alpha_x}{\sqrt{p_g}}|x\rangle, && \text{(A7)}\\
|\Psi_b\rangle &= \sum_{x\in X_b} \frac{\beta_x}{\sqrt{1-p_g}}|x\rangle. && \text{(A8)}
\end{aligned}$$

Similar to Grover's algorithm, each application of Q induces a rotation by an angle 2θ, moving the state closer from the initial state $|\Psi\rangle$ to the target state $|\Psi_g\rangle$, as illustrated in Figure A1.

* Corresponding author (email: zhouxu@tgqs.net)

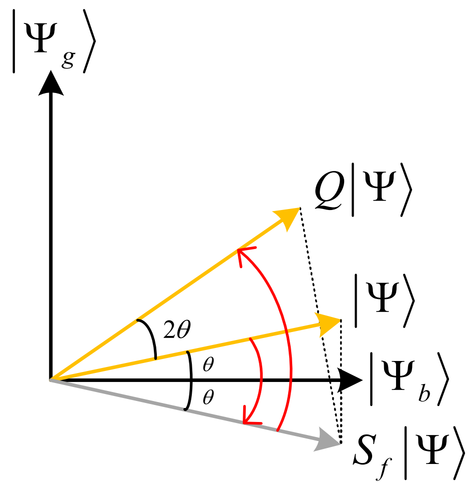

Figure A1 (Color online) Schematic illustration of the state evolution under the Q operator.

After r applications of Q, the state evolves to

$$|\Psi'\rangle = Q^r|\Psi\rangle = \sin\left((2r+1)\theta\right)|\Psi_g\rangle + \cos\left((2r+1)\theta\right)|\Psi_b\rangle. \tag{A9}$$

To ensure

$$\sin((2r+1)\theta) \approx 1, \tag{A10}$$

we require

$$(2r+1)\theta \approx \frac{\pi}{2}, \tag{A11}$$

leading to

$$r \approx \frac{\pi/2-\theta}{2\theta} = \frac{\pi}{4\theta} - \frac{1}{2}. \tag{A12}$$

Since r must be an integer, we choose

$$r = \left\lfloor \frac{\pi}{4\arcsin\left(\sqrt{p_g}\right)} \right\rfloor. \tag{A13}$$

This choice maximizes the success probability, which is given by

$$\sin^2\left(\left(2\left\lfloor \frac{\pi}{4\arcsin\left(\sqrt{p_g}\right)} \right\rfloor + 1\right)\arcsin\left(\sqrt{p_g}\right)\right) \approx 1. \tag{A14}$$

Appendix B Analysis of the EQAAA in subsection 2.2

The exact amplitude amplification operator EQ admits the following equivalent representations:

$$\begin{aligned} EQ &= \mathcal{A}R^{\phi}_{|0\rangle^{\otimes n}}\mathcal{A}^{\dagger}R^{\phi}_{f} && \text{(B1)}\\ &= \left(I^{\otimes n} + \left(e^{i\phi}-1\right)|\Psi\rangle\langle\Psi|\right)\left(I^{\otimes n} + \left(e^{i\phi}-1\right)|\Psi_g\rangle\langle\Psi_g|\right) && \text{(B2)}\\ &= e^{i\phi}\left[\cos\left(\frac{\alpha}{2}\right)I + i\sin\left(\frac{\alpha}{2}\right)\left(n_xX + n_yY + n_zZ\right)\right], && \text{(B3)} \end{aligned}$$

where the angle α and the components of the rotation axis are defined by

$$\alpha = 4\beta,\ \ \sin\beta = \sin\left(\frac{\phi}{2}\right)\sin\theta,\ \ \sin\theta = \sqrt{p_g}, \tag{B4}$$

and

$$n_x = \frac{\cos\theta}{\cos\beta}\cos\left(\frac{\phi}{2}\right), n_y = \frac{\cos\theta}{\cos\beta}\sin\left(\frac{\phi}{2}\right), n_z = \frac{\cos\theta}{\cos\beta}\cos\left(\frac{\phi}{2}\right)\tan\theta. \tag{B5}$$

Here, I, X, Y, Z denote the Pauli gates.

Within the three-dimensional space spanned by $\{|\Psi_g\rangle, |\Psi_b\rangle\}$, each application of EQ can be viewed as a rotation by an angle α around the axis $\vec{l} = [n_x, n_y, n_z]^T$, which gradually evolves the state from $|\Psi\rangle$ toward $|\Psi_g\rangle$. The total rotation angle is denoted by ω (see Figure B1), which satisfies

$$\cos\omega = \cos\left(2\arccos\left(\sin\left(\frac{\phi}{2}\right)\sqrt{p_g}\right)\right). \tag{B6}$$

It follows that

$$\omega = 2\arccos\left(\sin\left(\frac{\phi}{2}\right)\sqrt{p_g}\right) = 2\left(\frac{\pi}{2} - \arcsin\left(\sin\left(\frac{\phi}{2}\right)\sqrt{p_g}\right)\right). \tag{B7}$$

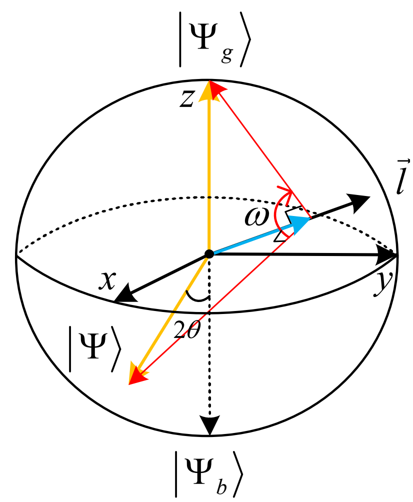

Figure B1 (Color online) Schematic illustration of the state evolution under the EQ operator.

After $J+1$ applications of EQ, to ensure the desired state $|\Psi_g\rangle$ is obtained with a theoretical success probability of 100%, the angle ω must satisfy

$$\omega = (J+1)\alpha = 4(J+1)\arcsin\left(\sin\left(\frac{\phi}{2}\right)\sqrt{p_g}\right). \tag{B8}$$

Equating (B7) and (B8) yields the condition

$$\sin\left(\frac{\pi}{4J+6}\right) = \sin\left(\frac{\phi}{2}\right)\sqrt{p_g}. \tag{B9}$$

Consequently, the phase angle ϕ is given by

$$\phi = 2\arcsin\left(\frac{\sin\left(\frac{\pi}{4J+6}\right)}{\sqrt{p_g}}\right). \tag{B10}$$

Appendix C Proof of Theorem 1

The correctness of DEQAAA relies on the exact amplitude amplification property of EQAAA (detailed in Appendix B). Different from traditional schemes, the exact amplitude amplification studied in this work only requires the total measurement probability of all target basis states to reach unity, without any constraint on preserving their relative amplitudes and relative phases.

In practical implementation, the whole highly entangled n-qubit system is approximately divided into several independent subsystems, and local EQAAA operations are performed in parallel on each divided subsystem. All local evolution results can be integrated into the global quantum state to realize unified state regulation, which is consistent with the circuit structure shown in Figure 3. Subsequently, the second phase of DEQAAA executes the standard global EQAAA on the obtained global state. Specifically, DEQAAA implements exact amplification after two phases, and the correctness analysis is conducted based on the value of p'_g (the global success probability after Phase 1), as follows:

Case 1: $p'_g = 1$

Case 1 corresponds to $p'_g = 1$, where $p'_g = \sum_{x\in X_g} P'(x)$ denotes the global success probability after Phase 1, and P' is the corresponding probability distribution of the state $|\Psi_1\rangle = \left(\bigotimes_{j=0}^{t-1} EQ_j^{J_j+1}\right)\mathcal{A}|0\rangle^{\otimes n}$.

The first distributed phase of DEQAAA is capable of raising the global success probability p'_g up to 1 for product states that satisfy node partition conditions and global target sets complying with $\prod_j |X_j| = |X_g|$, so exact amplitude amplification can be accomplished solely by the first stage. For general entangled states that fail to meet the above requirements, the second global phase remains necessary.

When $p'_g = 1$, $|\Psi_1\rangle$ already satisfies $\sum_{x \in X_g} |\langle x|\Psi_1\rangle|^2 = 1$, indicating that Phase 1 alone achieves global exact amplification. In this case, DEQAAA omits Phase 2, and the final state $|\Psi_2\rangle = |\Psi_1\rangle$ directly meets the requirement of $\sum_{x \in X_g} |\langle x|\Psi_2\rangle|^2 = 1$.

Case 2: $p'_g \neq 1$

Case 2 corresponds to $p'_g \neq 1$, where Phase 1 fails to amplify the success probability of $|\Psi_1\rangle$ to unity via parallel local exact amplitude amplification. To achieve global exact amplification, DEQAAA proceeds to Phase 2, first integrating the complete unitary operations of Phase 1 into a composite operator $\mathcal{B} = \left(\bigotimes_{j=0}^{t-1} EQ_j^{J_j+1}\right)\mathcal{A}$. The core of Phase 2 is the global exact amplitude amplification operator $\widehat{EQ} = \mathcal{B}R^{\hat{\phi}}_{|0\rangle^{\otimes n}}\mathcal{B}^\dagger R^{\hat{\phi}}_f$, whose form is fully consistent with EQAAA's core operator EQ. It is worth emphasizing that the conjugate transpose term $\mathcal{B}^\dagger$ in the operator still follows the distributed node architecture to complete the operation, which keeps consistent with the overall distributed design of the algorithm.

By setting the phase angle $\hat{\phi}$ and iteration count $\hat{J}$ to satisfy EQAAA's rotational angle condition (B9), $\hat{J}+1$ iterations of $\widehat{EQ}$ can exactly evolve the state $|\Psi_1\rangle$ to $|\Psi_2\rangle$. Here, $\hat{J} = \left\lfloor \frac{\pi}{4\arcsin\left(\sqrt{p'_g}\right)} - \frac{1}{2} \right\rfloor$ is determined by p'_g, ensuring the rotational evolution meets the exact amplification requirement.

The "Phase 1 + Phase 2" process is equivalent to the standard EQAAA process with $\mathcal{B}$ as the state preparation operator, whose correctness is guaranteed by EQAAA's exact amplification property. The final state $|\Psi_2\rangle$ thus satisfies $\sum_{x \in X_g} |\langle x|\Psi_2\rangle|^2 = 1$.

In summary, regardless of whether p'_g is 1 or not, DEQAAA can achieve exact amplitude amplification for the target strings $x \in X_g$, and the final state $|\Psi_2\rangle$ satisfies $\sum_{x \in X_g} |\langle x|\Psi_2\rangle|^2 = 1$.

Appendix D Proof of Theorem 2

The unitary operator $\mathcal{A}$ prepares an n-qubit state $|\Psi\rangle$ with an arbitrary amplitude distribution, and its implementation depth is defined as $\mathrm{dep}(\mathcal{A})$.

Without loss of generality, let p_g be the probability of measuring a target string in the global target set X_g, and $|X_g|$ the number of target strings in X_g.

In QAAA, the amplitude amplification operator is defined as $Q = \mathcal{A}S_{|0\rangle^{\otimes n}}\mathcal{A}^\dagger S_f$, which is executed repeatedly r times, where r is given by:

$$r = \left\lfloor \frac{\pi}{4\arcsin\left(\sqrt{p_g}\right)} \right\rfloor. \tag{D1}$$

For simplicity, the circuit depth of the $C^{n-1}Z$ gate is defined as 1. From this, the depth of S_f (for $|X_g|$ targets) is $\mathrm{dep}(S_f) = 3|X_g|$, and the depth of $S_{|0\rangle^{\otimes n}}$ is $\mathrm{dep}(S_{|0\rangle^{\otimes n}}) = 3$.

The total depth of QAAA is the sum of the initial state preparation depth and the depth of r repeated Q operations. Thus, the total depth is

$$\begin{aligned} \mathrm{dep}(\mathrm{QAAA}, p_g, |X_g|) &= \mathrm{dep}(\mathcal{A}) + r \cdot (3|X_g| + 2\mathrm{dep}(\mathcal{A}) + 3) && \text{(D2)} \\ &= (2r+1) \cdot \mathrm{dep}(\mathcal{A}) + r \cdot (3|X_g| + 3). && \text{(D3)} \end{aligned}$$

This completes the proof.

Appendix E Proof of Theorem 3

Following the basic definitions in Theorem 2, the implementation depth of the unitary operator $\mathcal{A}$ is $\mathrm{dep}(\mathcal{A})$; p_g denotes the probability of measuring a target string in the global target set X_g, and $|X_g|$ is the number of target strings in X_g.

In EQAAA, the exact amplitude amplification operator is defined as $EQ = \mathcal{A}R^{\phi}_{|0\rangle^{\otimes n}}\mathcal{A}^\dagger R^{\phi}_f$, which is iteratively applied $J+1$ times, with J given by:

$$J = \left\lfloor \frac{\pi}{4\arcsin\left(\sqrt{p_g}\right)} - \frac{1}{2} \right\rfloor. \tag{E1}$$

Similar to the $C^{n-1}Z$ gate, the circuit depth of the $C^{n-1}\mathrm{PS}(\phi)$ gate is defined as 1 for simplicity. From this, the depth of R^{ϕ}_f (for $|X_g|$ targets) is $\mathrm{dep}(R^{\phi}_f) = 3|X_g|$, and the depth of $R^{\phi}_{|0\rangle^{\otimes n}}$ is $\mathrm{dep}(R^{\phi}_{|0\rangle^{\otimes n}}) = 3$, which is consistent with the depths of S_f and S_0.

The total depth of EQAAA is the sum of the initial state preparation depth and the depth of $J+1$ repeated EQ operations. Thus, the total depth is

$$\begin{aligned} \mathrm{dep}(\mathrm{EQAAA}, p_g, |X_g|) &= \mathrm{dep}(\mathcal{A}) + (J+1) \cdot (3|X_g| + 2\mathrm{dep}(\mathcal{A}) + 3) && \text{(E2)} \\ &= (2J+3) \cdot \mathrm{dep}(\mathcal{A}) + (J+1) \cdot (3|X_g| + 3)\,. && \text{(E3)} \end{aligned}$$

This completes the proof.

Appendix F Proof of Theorem 4

Following the basic definitions in Theorem 2 and Theorem 3, the global target set is X_g (with $|X_g|$ target strings), and the distributed architecture contains t nodes; the j-th node has a local target set X_j (with $|X_j|$ target strings), a success measurement probability p_j, and the implementation depth of the corresponding local unitary preparation operator $\mathcal{A}_{|\varphi_j\rangle}$ (generating substate $|\varphi_j\rangle = \mathcal{A}_{|\varphi_j\rangle}|0\rangle^{\otimes n_j}$) is $\mathrm{dep}(\mathcal{A}_{|\varphi_j\rangle})$. The global initial state is prepared by the unitary operator $\mathcal{A}$, with depth $\mathrm{dep}(\mathcal{A})$.

The subsequent proof will derive the circuit depths of the first phase (local execution of distributed nodes) and the second phase (global exact amplification) respectively, and finally integrate to obtain the total depth of DEQAAA.

Phase 1: local execution of distributed nodes

The first phase is the local execution phase of distributed nodes, where each node independently performs local EQAAA operations. The core is the dedicated exact amplitude amplification operator EQ_j (defined in (25)), which consists of local phase rotation operators $R_{f_j}^{\phi_j}$, $R_{|0\rangle^{\otimes n_j}}^{\phi_j}$, and $\mathcal{A}_{|\varphi_j\rangle}$ and its inverse, with the phase angle ϕ_j calculated by (29).

The EQ_j operator is iteratively applied J_j+1 times, with the iteration count J_j given by

$$J_j = \left\lfloor \frac{\pi}{4\arcsin\left(\sqrt{p_j}\right)} - \frac{1}{2} \right\rfloor, \tag{F1}$$

consistent with the global iteration logic of EQAAA. Referring to the depth definition logic in Theorem 3, the depth of the $C^{n-1}\mathrm{PS}(\phi)$ gate is defined as 1. Since the local phase rotation operators $R_{f_j}^{\phi_j}$ and $R_{|0\rangle^{\otimes n_j}}^{\phi_j}$ are both constructed based on the $C^{n_j-1}\mathrm{PS}(\phi_j)$ gate, their depths are both set to 1. Thus, the operation depth of the j-th node is

$$\mathrm{dep}(j\text{-th node}, p_j, |X_j|) = (J_j+1)\cdot\left(3|X_j| + 2\mathrm{dep}(\mathcal{A}_{|\varphi_j\rangle}) + 3\right), \tag{F2}$$

which matches the corresponding formula in the theorem. Its depth composition logic is fully consistent with that of the global operator in EQAAA, i.e., the total depth is the sum of the depths of J_j+1 iterations of the single EQ_j operator.

As each node performs local operations in parallel, the total depth of the first phase is the sum of the global initial state preparation depth and the maximum operation depth among all nodes, i.e.,

$$\mathrm{dep}(\text{First phase}) = \mathrm{dep}(\mathcal{A}) + \max_{j\in\{0,1,\cdots,t-1\}} \{\mathrm{dep}(j\text{-th node}, p_j, |X_j|)\}. \tag{F3}$$

Phase 2: global exact amplification

After the first phase, the system state evolves to $|\Psi_1\rangle$, and its global success probability (i.e., the success probability of the second phase) is defined as

$$p_g' = \sum_{x\in X_g} P'(x), \tag{F4}$$

where P' is the exact probability distribution corresponding to $|\Psi_1\rangle$. The second phase is global exact amplification, executed only when $p_g' \neq 1$. In this case, the first phase cannot amplify the success probability of $|\Psi_1\rangle$ to 1 (failing to achieve global exact amplification), requiring correction via global exact amplitude amplification operations.

In this phase, the complete unitary operation of the first phase is first encapsulated into a composite operator

$$\mathcal{B} = \left[\bigotimes_{j=0}^{t-1}\left(EQ_j^{J_j+1}\right)\right]\mathcal{A}, \tag{F5}$$

with the core being the global exact amplitude amplification operator

$$\widehat{EQ} = \mathcal{B}R_{|0\rangle^{\otimes n}}^{\hat{\phi}}\mathcal{B}^{\dagger}R_f^{\hat{\phi}}. \tag{F6}$$

The iteration count

$$\hat{J} = \left\lfloor \frac{\pi}{4\arcsin\left(\sqrt{p_g'}\right)} - \frac{1}{2} \right\rfloor, \tag{F7}$$

which is consistent with the iteration logic of J in Theorem 3.

Referring to the depth derivation logic of Theorem 3, $\mathrm{dep}(\mathcal{B}) = \mathrm{dep}(\text{First phase})$ and $\mathrm{dep}(\mathcal{B}^{\dagger}) = \mathrm{dep}(\mathcal{B})$ (the depth of an operator is equal to that of its inverse). The depths of global phase rotation operators are consistent with EQAAA: the depth of $R_f^{\hat{\phi}}$ is $3|X_g|$, and the depth of $R_{|0\rangle^{\otimes n}}^{\hat{\phi}}$ is 3. Thus, the depth of a single $\widehat{EQ}$ iteration is $3|X_g| + 2\mathrm{dep}(\text{First phase}) + 3$, and the total depth of the second phase is

$$\mathrm{dep}(\text{Second phase}) = \left(\hat{J}+1\right)\cdot\left(3|X_g| + 2\mathrm{dep}(\text{First phase}) + 3\right). \tag{F8}$$

In summary, the total circuit depth of DEQAAA is determined by the value of p_g':

When $p_g' = 1$, the local exact amplitude amplification executed in parallel in the first phase suffices to achieve exact amplification of the global target state, and the total depth is the depth of the first phase, i.e.,

$$\mathrm{dep}(\text{DEQAAA}) = \mathrm{dep}(\text{First phase}). \tag{F9}$$

When $p'_g \neq 1$, global exact amplification in the second phase is required to correct deviations, and the total depth is the sum of the depths of the two phases, i.e.,

$$\mathrm{dep}(\mathrm{DEQAAA}) = \mathrm{dep}(\text{First phase}) + \mathrm{dep}(\text{Second phase}). \tag{F10}$$

Thus, the circuit depth of DEQAAA satisfies (47), and the theorem is proven.

Appendix G The decomposition of $C^3PS(\phi)$ in subsection 5.5

In the above experiments, QAAA achieves phase flip using C^3Z gates, whereas EQAAA and DEQAAA realize phase rotation through $C^3PS(\phi)$ gates. Note that the C^3Z gate is a special case of the $C^3PS(\phi)$ gate with $\phi = \pi$, i.e., $C^3Z = C^3PS(\pi)$.

However, current quantum computers generally do not support the direct implementation of such complex multi-controlled gates. A more common approach is to decompose them into equivalent combinations of single-qubit and two-qubit gates.

The decomposition of the $C^3PS(\phi)$ gate was also discussed in Ref. [1]. Nevertheless, this method requires the execution of multiple CPS and CNOT gates. Since two-qubit gates like these are inherently more challenging to implement with high fidelity than single-qubit operations, they significantly increase the practical complexity of the circuit. Furthermore, as the number of qubits n increases, this approach adopts the technique outlined in Lemma 7.5 of Ref. [2]. A notable drawback of this method is that it further necessitates the decomposition of multi-controlled X gates, thereby introducing an additional layer of complexity and resource overhead.

To enhance the implementation efficiency of multi-controlled phase gates on NISQ devices, we propose an improved decomposition scheme. This scheme constructs a deterministic quantum circuit that expresses the gate as an optimized sequence of elementary single-qubit gates and CNOT gates.

Specifically, we present an enhanced decomposition scheme that implements the $C^3PS(\phi)$ gate. This method naturally generalizes to arbitrary n-qubit controlled-phase gates ($C^{n-1}PS(\phi)$), though the detailed derivation is not included in this paper.

Lemma G1 (**Decomposition of** $C^3PS(\phi)$) For any single-qubit unitary gate $PS(\phi)$, the $C^3PS(\phi)$ gate can be decomposed into the quantum circuit depicted in Figure G1, where ϕ denotes the phase angle and $n = 4$ is the total number of qubits involved in the $C^3PS(\phi)$ gate.

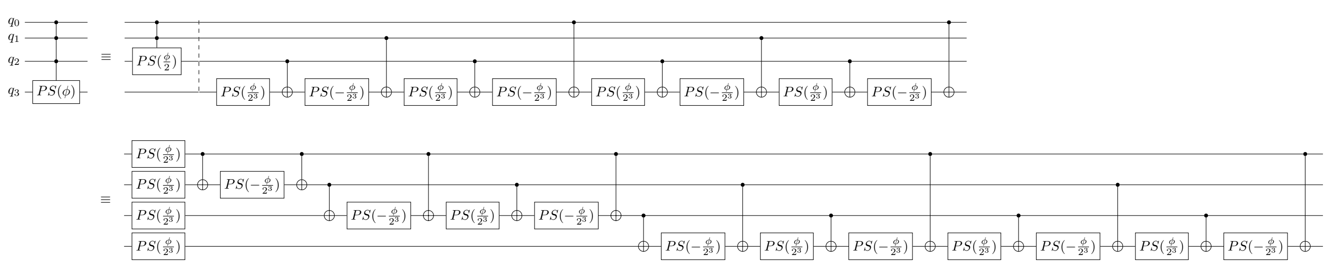

Figure G1 Quantum circuit for the decomposition of $C^3PS(\phi)$ gate.

Proof. It is straightforward to confirm that the unitary matrices associated with the quantum circuits on both sides of the equality sign are equivalent.

References

1 Zhou X, Xu X S, Zheng S G, Luo L. Distributed exact generalized Grover's algorithm. Front Comput Sci, 2025, 20: 2007905
2 Barenco A, Bennett C H, Cleve R, DiVincenzo D P, Margolus N, Shor P, Sleator T, Smolin J A, Weinfurter H. Elementary gates for quantum computation. Phys Rev A, 1995, 52: 3457